Fluorinated Alcohols' Effects on Lipid Bilayer Properties

Mike Zhang,[1,2] Thasin Peyear,[1] Ilias Patmanidis,[3] Denise V. Greathouse,[4] Siewert J. Marrink,[3] Olaf S. Andersen,[1,*] and Helgi I. Ingólfsson[1,3,5,*]

[1]Department Physiology and Biophysics, Weill Cornell Medicine, New York City, New York; [2]The Bronx High School of Science, New York City, New York; [3]Groningen Biomolecular Science and Biotechnology Institute and Zernike Institute for Advanced Materials, University of Groningen, Groningen, the Netherlands; [4]Department of Chemistry and Biochemistry, University of Arkansas, Fayetteville, Arkansas; and [5]Biosciences and Biotechnology Division, Physical and Life Sciences Directorate, Lawrence Livermore National Laboratory, Livermore, California

ABSTRACT   Fluorinated alcohols (fluoroalcohols) have physicochemical properties that make them excellent solvents of peptides, proteins, and other compounds. Like other alcohols, fluoroalcohols also alter membrane protein function and lipid bilayer properties and stability. Thus, the questions arise: how potent are fluoroalcohols as lipid-bilayer-perturbing compounds, could small residual amounts that remain after adding compounds dissolved in fluoroalcohols alter lipid bilayer properties sufficiently to affect membranes and membrane protein function, and do they behave like other alcohols? To address these questions, we used a gramicidin-based fluorescence assay to determine the bilayer-modifying potency of selected fluoroalcohols: trifluoroethanol (TFE), HFIP, and perfluoro-*tert*-butanol (PFTB). These fluoroalcohols alter bilayer properties in the low (PFTB) to high (TFE) mM range. Using the same assay, we determined the bilayer partitioning of the alcohols. When referenced to the aqueous concentrations, the fluoroalcohols are more bilayer perturbing than their nonfluorinated counterparts, with the largest fluoroalcohol, PFTB, being the most potent and the smallest, TFE, the least. When referenced to the mole fractions in the membrane, however, the fluoroalcohols have equal or lesser bilayer-perturbing potency than their nonfluorinated counterparts, with TFE being more bilayer perturbing than PFTB. We compared the fluoroalcohols' molecular level bilayer interactions using atomistic molecular dynamics simulations and showed how, at higher concentrations, they can cause bilayer breakdown using absorbance measurements and ^{31}P nuclear magnetic resonance.

INTRODUCTION

Fluorinated alcohols (fluoroalcohols) such as trifluoroethanol (2,2,2-trifluoroethanol; TFE), hexafluoroisopropanol (1,1,1,3,3,3-hexafluoro-2-propanol; HFIP), and perfluoro-*tert*-butanol (1,1,1,3,3,3-hexafluoro-2-(trifluoromethyl)-2-propanol; PFTB) are used extensively as solvents, cosolvents, and additives in synthetic chemistry (1,2). Their tendency to disrupt native oligomeric protein structures and induce α-helical structure in proteins and peptides similarly make them useful in biochemical and spectroscopic studies (3,4), in which fluoroalcohols have been used to unfold aggregates of the Alzheimer's amyloid-β (Aβ) peptides

(5), incorporate peptides into lipid bilayers (6,7), and dissociate KcsA tetramers (8). Like other alcohols (see (9–12) and references therein), fluoroalcohols also alter membrane protein function. At low-to-mid mM concentrations, fluoroalcohols modulate the function of P2X receptors (13), nicotinic acetylcholine receptors (14), the mechanosensitive channel of small conductance (15), KcsA channels (16), and Kv1.3 potassium channels (17). At higher concentrations, the fluoroalcohols' effects on lipid bilayer properties per se have been described in previous studies, in which they produce bilayer leakage, reduce the lipid acyl chain order, alter the lipid phase transition temperature, and induce micellar aggregation (8,18,19). It remains unclear, however, whether the changes in membrane protein function observed at the lower concentrations also could result from changes in lipid bilayer properties.

Indeed, HFIP has been shown to increase ion movement across lipid bilayers at low mM concentrations (20), which

may lead to complications in functional assays, such as whether Aβ-oligomer produces gradual increases in bilayer conductance or discrete channels (17,20,21). Similarly, Wang et al. (22) cautioned against the use of HFIP when studying membrane-induced fibrillogenesis because they found it decreases the rate of human islet amyloid polypeptide fibrillation at lipid bilayer interfaces.

Compared to their nonfluorinated counterparts, fluoroalcohols have higher vapor pressures (Table S1), but it is nevertheless difficult to remove them completely (20). It therefore becomes important to know the fluoroalcohols' bilayer-modifying potencies and the concentrations at which they would be expected to become indiscriminate modifiers of membrane protein function.

To quantify the bilayer-modifying potency of commonly used fluoroalcohols as sensed by a bilayer-spanning ion channel, we used a calibrated gramicidin-based assay. Gramicidin channels are miniproteins formed by the transmembrane dimerization of nonconducting subunits residing in opposing bilayer leaflets (23,24). The channels are selective for monovalent cations, and the channel length is usually less than the bilayer thickness, meaning that lipids adjacent to the channel have to reorganize as the channel forms (Fig. 1 A). This reorganization of the surrounding bilayer causes the gramicidin monomer ↔ dimer equilibrium to be energetically coupled to the cost of deforming the bilayer (24–26), which becomes the bilayer contribution to the free energy of dimerization. Changes in gramicidin channel activity thus serve as a readout for measuring changes in lipid bilayer properties (26,27), and the changes in bilayer properties that alter the gramicidin monomer ↔ dimer equilibrium also alter the function of channels formed by integral membrane proteins (28–31).

Gramicidin-based assays are sensitive to changes in all bilayer properties that alter the energetic cost of bilayer deformations (e.g., bilayer thickness and intrinsic curvature and the associated elastic compression and bending moduli), as well as changes to the boundary between the channel and the bilayer, but not changes in bilayer properties that do not alter the gramicidin monomer ↔ dimer equilibrium such as membrane fluidity (see (32)). The assays can be implemented using both single-channel methods (24) and fluorescence quench methods (33,34), and there is good agreement between the results obtained using these methods (12). Moreover, because the assay is functional, using membranes with a hydrophobic thickness that much larger than the channels' hydrophobic length (such that the bilayer-channel hydrophobic mismatch and the bilayer deformation energy are large), it is sensitive to small changes in lipid bilayer properties (30,33).

We therefore used a calibrated gramicidin-based fluorescence assay (33,34) to quantify the bilayer-modifying potencies of three fluoroalcohols (TFE, HFIP, and PFTB), compared them to their nonfluorinated counterparts, and explored their tendency to disrupt lipid bilayers. To relate the alcohols' bilayer-modifying potency to their molar ratio in the bilayer, we also determined their bilayer/aqueous phase partition coefficients by determining the fluoroalcohols' bilayer-modifying effects at different lipid concentrations. The alcohols' bilayer interactions also were explored at the molecular level using atomistic molecular dynamics (MD) simulations of the fluorinated alcohols and nonfluorinated counterparts in model bilayers. Finally, the fluoroalcohols' ability to disrupt membrane integrity was assessed using absorbance measurements and ^{31}P nuclear magnetic resonance (NMR).
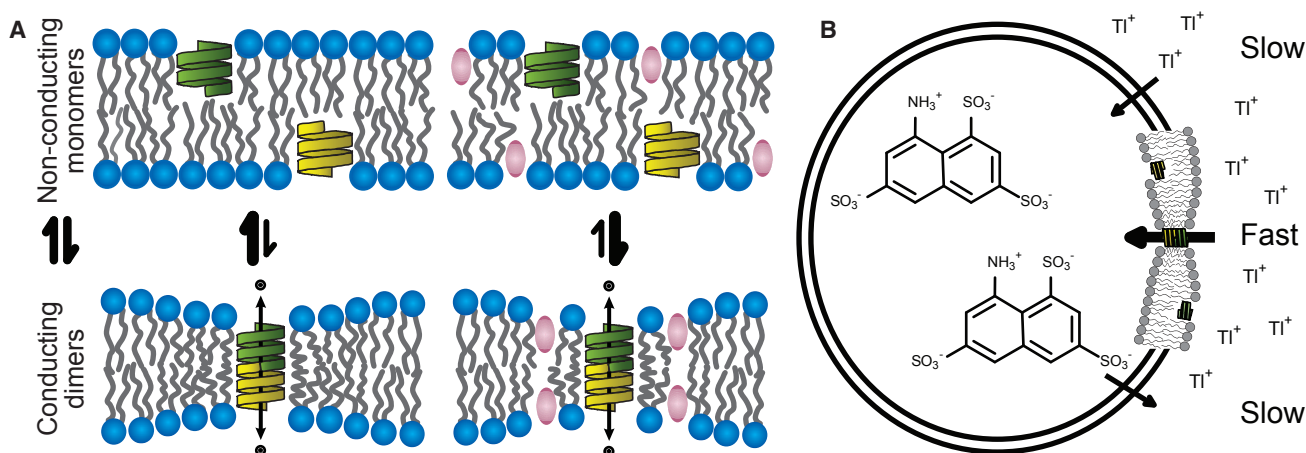

FIGURE 1 Gramicidin-based fluorescence quench assay. (A) A schematic depiction of gramicidin channel formation in lipid bilayers is shown. Gramicidin monomers from opposing bilayer leaflets dimerize to form a cation-conducting channel. The channel is shorter than the surrounding bilayer, and the bilayer deforms around the channel, making gramicidin channel formation rate and lifetime sensitive to bilayer properties. (B) The gramicidin-based fluorescence assay uses fluorophore-loaded large unilamellar vesicles (LUVs) doped with gramicidin and measures the rate of fluorescence decay as the gramicidin-channel-permeable quencher enters the vesicles. The quencher Tl^+ and the fluorophore ANTS cross the lipid bilayer poorly, whereas gramicidin channels are readily Tl^+ permeable. To see this figure in color, go online.

MATERIALS AND METHODS

Materials

Alcohols of the highest available purity were obtained from Sigma-Aldrich (St. Louis, MO); all lipids were from Avanti Polar Lipids (Alabaster, AL). The gramicidin was the naturally occurring mixture of gramicidins A, B, and C that is produced by *Brevibacillus brevis*, which was from Sigma-Aldrich. Historically, this mixture has been called gramicidin D (gD) after R. Dubos, who discovered the gramicidins (25); it contains 80–85% [Val^1]gA (26). We determined the alcohols' bilayer-modifying potency using a gramicidin-based fluorescence assay described previously (33,34). In short, large unilamellar lipid vesicles (LUVs) loaded with the water-soluble fluorophore, 8-aminonaphthalene-1,3,6-trisulfonic acid (ANTS; Invitrogen, Eugene, OR) were made of 1,2-dierucoyl-*sn*-glycero-3-phosphocholine (DC$_{22:1}$PC) using a mixture of hydration (in 140 mM NaNO$_3$, 10 mM HEPES (pH 7.0)), sonication, freeze-thawing, and miniextrusion through 100 nm polycarbonate filters. (The long-chain lipids increase the bilayer thickness sufficiently to shift the gramicidin monomer ↔ dimer equilibrium toward the nonconducting monomers, which facilitates the detection of changes in the monomer ↔ dimer equilibrium.) External ANTS was removed using a PD-10 Desalting Column from GE Healthcare (Piscataway, NJ). The size distribution was determined by dynamic light scattering using an Anton Paar (Graz, Austria) Litesizer 500 particle analyzer, which showed a single peak with an average particle radius of ~130 nm and a polydispersity index of ~10%. For the experiments at pH 4.0 (rather than pH 7.0), the solutions were buffered with 10 mM Glycyl-glycine (Gly-Gly) instead of HEPES.

Bilayer-modifying potency quantified with fluorescence quench experiments

These experiments were done with gramicidin-containing and gramicidin-free LUVs. 260 nM gramicidin was added to ANTS-loaded LUVs (lipid/gramicidin monomer ratio ~1000:1) 24 h before use, and the mixture was incubated at 12°C in the dark. For the experiments, the LUV suspension was incubated with the alcohol to be studied for 10 min at 25°C. The vesicle-entrapped ANTS was quenched by the gramicidin channel permeable quencher (Tl$^+$), and the LUV solution was mixed with the quench buffer (50 mM TlNO$_3$, 94 mM NaNO$_3$, 10 mM HEPES (pH 7.0)) in a SX.20 stopped-flow spectrofluorometer (Applied Photophysics, Leatherhead, UK) to measure the time course of fluorescence quenching. The excitation wavelength was 352 nm, the fluorescence emission above 455 nm was recorded, and the fluorescence signal was normalized to that measured in the absence of the quencher. The unavoidable variation in LUV sizes means that the quencher influx cannot be described by a single exponential decay, and the results for the first 2−100 ms were analyzed using a stretched exponential fit (35):

$$F(t) = F(\infty) + (F(0) - F(\infty)) \times exp\left\{ -\left(\frac{t}{\tau_0}\right)^\beta \right\}, \tag{1}$$

where $F(t)$ is the fluorescence at time t, τ_0 a parameter with units of time, and β ($0 < \beta \leq 1$) a measure of the sample dispersity. The fluorescence quench rate at 2 ms then was calculated as

$$k(t) = (\beta/\tau_0) \times (t/\tau_0)^{\beta-1}. \tag{2}$$

We quantified each alcohol's bilayer-modifying potency in terms of the concentration at which the alcohol doubled the fluorescence quench rate (D), which we determined by fitting a linear relation

$$f([alc]) = 1 + [alc]/D, \tag{3}$$

where $f[alc]$ denotes the fluorescence quench rate at alcohol concentration [alc] to the increases in the quench rate (normalized to control, in the absence of alcohol) as a function of the alcohol concentration.

Alcohol partitioning determined from fluorescence quench experiments

Alcohol (alc) partitioning into lipid bilayers denotes partitioning between two immiscible phases, the aqueous phase and the membrane phase (36). The quantitative relation between the concentration of alcohol in the membrane phase (expressed as moles/volume, [alc]$_m$), and the aqueous concentration [alc]$_{aq}$ can be described using different frameworks (37). For this analysis, it is convenient to use a bulk partition description:

$$[alc]_m = K_p \times [alc]_{aq}, \tag{4}$$

where K_p is the (dimensionless) partition coefficient.

When an alcohol is added to the aqueous solution bathing a lipid bilayer, to a nominal concentration [alc]$_{nom}$, the alcohol will partition between the aqueous and membrane phases (38–40). The aqueous and membrane alcohol concentrations are estimated from Eq. 4 together with the conservation relation:

$$[alc]_{nom} \times V_{aq} = [alc]_{aq} \times V_{aq} + [alc]_m \times V_{lip}, \tag{5}$$

where V_{aq} and V_{lip} denote the volumes of the aqueous and lipid solutions, respectively (and we assume $V_{aq} \gg V_{lip}$). We thus find, using Eq. 4, that

$$[alc]_{aq} = [alc]_{nom} \times \frac{V_{aq}}{\left(V_{aq} + K_p \times V_{lip}\right)}$$
$$= [alc]_{nom} \times \frac{1}{\left(1 + K_p \times r_{lip}\right)} \tag{6}$$

and

$$[alc]_m = [alc]_{nom} \times \frac{K_p \times V_{aq}}{\left(V_{aq} + K_p \times V_{lip}\right)}$$
$$= [alc]_{nom} \times \frac{K_p}{\left(1 + K_p \times r_{lip}\right)}, \tag{7}$$

where $r_{lip} = V_{lip}/V_{aq}$.

The alcohol mole-fraction in the bilayer (m_{alc}) then becomes

$$m_{alc} = \frac{[alc]_m}{\left([alc]_m + [lip]_m\right)}$$
$$= \frac{[alc]_{nom} \times K_p}{[alc]_{nom} \times K_p + \left(1 + K_p \times r_{lip}\right) \times [lip]_m}, \tag{8}$$

where the molar lipid concentration in the membrane phase ([lip]$_m \approx 1.1$ M) was estimated following Ingólfsson and Andersen (12). That is, [alc]$_{aq}$ and m_{alc} will decrease with increasing r_{lip}, which provides a method to estimate K_p from the changes in fluorescence quench rate as a function of the amount of lipid in the incubation mixture (i.e., as a function of r_{lip}). The basic assumption here is that the changes in the relative fluorescence rate (R) reflect changes in [alc]$_m$ and that the relation between R and [alc]$_m$ can be expressed as (12)

$$R = 1 + [\text{alc}]_{\text{nom}} \times \frac{1}{\left(1 + K_{\text{p}} \times r_{\text{lip}}\right) \times D_{\text{aq}}}$$

$$= 1 + [\text{alc}]_{\text{nom}} / D_{\text{nom}}, \quad (9)$$

where D_{aq} and D_{nom} denote the actual and nominal aqueous alcohol concentrations when $R = 2$.

We can thus determine K_{p} from the changes in D_{nom} as a function of r_{lip} using the following expression:

$$D_{\text{nom}} = D_{\text{aq}}\left(1 + K_{\text{p}} \times r_{\text{lip}}\right). \quad (10)$$

The lipid volume (V_{lip}) in the fluorescence quench experiments was varied between 0.12 and 0.97 μL per mL total volume. For each alcohol, D was determined for a range of lipid volumes, i.e., r_{lip}, as described above. K_{p} then was determined by fitting Eq. 9 to the lipid volumes and their respective D using the jackknife method (41) for error estimation. (In the jackknife method, the first repeat for one of the lipid volume was removed from the set, and all of the doubling concentrations (Ds) were calculated and fitted to the equation above for the partition coefficient. Then the second repeat was removed, and another partition coefficient was obtained from the fit; this continued until the nth repeat had been removed, and the partition coefficient (mean $\pm$ SD) was calculated from the set.)

Alcohol bilayer interaction explored with MD

The MD simulations were performed using the GROMACS 4.6.7 simulation package (42) and the GROMOS 53A63 united-atom force field (43). 1,2-dioleoyl-*sn*-glycero-3-phosphocholine (DOPC) lipid topologies were generously provided by Alex H. Vries (available on request); the topologies for the normal alcohols as well as the fluoroalcohols were from the automated force field topology builder (ATB) (44), with ATB molids: ethanol 23009, 2-propanol 3488, *tert*-butanol 843, TFE 1655, HFIP 6187, and PFTB 28298. All systems contained 578 lipids and were solvated in SPC water (45) (>60 waters per lipid). The number of alcohol molecules and counter ions (Na$^+$ and Cl$^-$) was set to 10 ± 1 mol% alcohol in the bilayer phase and 150 mM NaCl. The temperature was coupled individually for the solvent and the bilayer to increase the stability of the system. More specifically, the temperature was kept constant at 298 K by using a Berendsen thermostat with a time constant of 0.1 ps (46). The pressure was maintained at 1.0 bar by coupling the system to a semi-isotropic pressure bath (isotropic along the x and y axes but different along the z axis) using the Berendsen barostat with a time constant of 0.5 ps and compressibility of 4.6×10^{-5} bar^{-1} (46). The partial mesh Ewald method (47) was employed for electrostatic and van der Waals interactions. The Coulomb cutoff distance was set to 1.4 nm, and the short-range neighbor list cutoff was set to 0.9 nm. The LINCS algorithm (48) was used to constrain the length of all bonds. The time step for integration was 2 fs. Energy minimization was done using the "Steepest Descent" algorithm, and all systems were equilibrated by gradually removing restraints for 400 ps before producing trajectories of ~350 ns.

The last 100 ns of each trajectory were used for analysis. The bilayer thickness was measured as the average distance between the DOPC phosphates in the opposing bilayer leaflets and the area per lipid as the average bilayer area divided by the number of lipids per leaflet. The average acyl chain order is the average second-rank order parameter (P_2) for the lipid acyl chain. P_2 was calculated from the angle θ between the bilayer normal (approximated as the z axis) and the vector along each bond in the lipid tails, as $P_2 = (1/2)(3 \cos^2(\theta-1))$. The alcohol angle with respect to the bilayer was approximated as the angle between the alcohols' oxygen-central carbon vector with respect to the box z axis.

Changes in membrane organization determined using vesicle absorbance

The vesicle light absorbance was used to estimate lipid vesicle integrity. Concentrated lipid vesicle solutions are turbid due to light scattering, and the turbidity will change when the vesicle organization is disrupted (49–51) and decrease to near zero if the disruption is so extreme as to cause dissolution of the vesicles. To test whether the fluoroalcohols disrupted the membrane organization, we measured the absorbance of multilamellar vesicle (MLV) suspensions (2 mM lipid in 140 mM NaNO$_3$, 10 mM HEPES (pH 7.0)) at increasing alcohol concentrations. The absorbance between 400 and 450 nm was measured using an Aquamate Spectrophotometer (Thermo Scientific, Waltham, MA) and normalized to the absorbance in the absence of the alcohol. The MLVs were made as above but without the miniextrusion step and without the fluorophore from DOPC, 1,2-dieico-senoyl-*sn*-glycero-3-phosphocholine (DC$_{20:1}$PC), and DC$_{22:1}$PC.

Membrane organization determined using ^{31}P NMR

To better understand the changes in membrane organization that underlie the changes in absorbance, we used phosphorus (^{31}P) NMR spectroscopy on MLVs. MLVs were prepared by drying lipid (40 μmol DOPC) from chloroform stock solution under a stream of N$_2$ gas and further under vacuum (<40 mTorr) for 48 h to remove traces of solvent. The lipid film was resuspended in 10 mM HEPES, 70 mM NaNO$_3$ (pH 7.0) (typically 0.4 mL was used; 1 mL was used to accommodate the smaller volumes of HFIP and TFE required for the 10 and 20 mM samples). The excess volume was removed after centrifugation (see below). The samples were subjected to several heat-thaw cycles (heat at 50°C, thaw at 4°C; in 5, 10, 20, 30, and 60 min intervals) with 1 min vortexing between each cycle. After the final cycle, TFE or HFIP was added (to final concentrations ranging from 10 to 200 mM), and the suspension was gently vortexed and allowed to incubate 50°C for 10 min. The lipid-solvent suspensions were transferred to 5 mm glass tubes and centrifuged at 10,000 rotations per minute (12,000 $\times$ g) for 2 h at 4°C. The supernatant was removed, the hydrated pellet was flushed with N$_2$ gas, and the tube was sealed with a rubber stopper and epoxy. Lipid-only MLVs were prepared in the same manner except without the addition of solvent. Phosphorus NMR spectra were recorded within 18 h of preparing the MLVs.

^{31}P NMR spectra were acquired on a Bruker (Billerica, MA) Avance 300 spectrometer using the Bruker zgpg pulse program with 256 scans, a 6 μs 90° pulse, and a recycle delay time of 5 s. Measurements were performed in a Doty 8 mm wideline probe (Doty Scientific, Columbia, SC) with broadband 1H decoupling at 50°C. Before Fourier transformation, an exponential weighting function with 200 Hz line broadening was applied. The chemical shifts were referenced externally to 85% phosphoric acid at 0 ppm.

RESULTS AND DISCUSSION

We determined the bilayer-perturbing potencies of the three fluoroalcohols (TFE, HFIP, and PFTB) and their nonfluorinated counterparts in DC$_{22:1}$PC lipid bilayers using a gramicidin-based fluorescence quench assay (33,34). The assay reports changes in the overall gramicidin channel activity by quantifying the changes in the rate of influx (the quench rate) of the gramicidin-channel-permeable Tl$^+$ into fluorophore-loaded LUVs (the basic principle of the assay is illustrated in Fig. 1 *B*).

Fig. 2 *A* shows fluorescence time courses observed in the absence and presence of HFIP. In LUVs without gramicidin and no added HFIP, the fluorescence stays almost constant
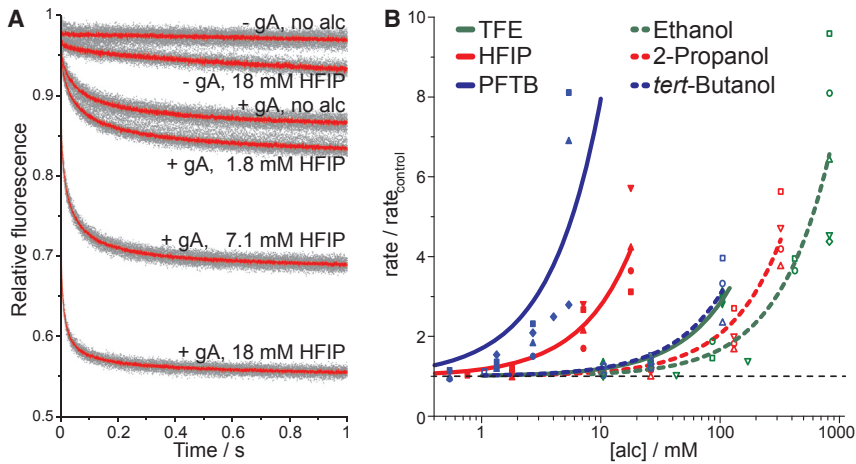
FIGURE 2 Fluorinated alcohols' bilayer-perturbing effect as determined using the gramicidin-based fluorescence assay. (*A*) Normalized fluorescence time courses observed with fluorophore-loaded LUVs incubated with varying [HFIP] are shown, with and without added gramicidin. Average traces (*red lines*) and within-sample repeats (>7 per condition; *gray dots*) over 1 s are shown. (*B*) The relative changes in quench rate, at pH 7.0, for the fluoroalcohols (*filled symbols*) and their nonfluorinated counterparts (*open symbols*, from (12)) are shown. The dotted line represents no change, and the solid lines are fits of $f([alc]) = 1 + [alc]/D$ to the results; the differently shaped symbols for each alcohol denote different days of experiments. To see this figure in color, go online.

over the 1 s observation period (Fig. 2 *A*, *top curve*), indicating that there is minimal influx of Tl^+ into the LUVs (Tl^+ may cross the bilayer in the form of $TlNO_3$ ion pairs (52)). Addition of 18 mM HFIP (the highest concentration tested) caused a slight increase in the fluorescence quench rate, indicating that HFIP at this concentration increases the quencher influx through the bilayer (Fig. 2 *A*, *second curve* from the *top*). In the presence of gramicidin, in which some LUVs would have one or more conducting gramicidin channels, the fluorescence quench rate was increased, indicating an increased quencher influx (Fig. 2 *A*, *third curve* from the *top*). Further increases in the [HFIP] produced faster fluorescence quench rates (faster quencher influx), demonstrating that HFIP shifted the gramicidin monomer $\leftrightarrow$ dimer equilibrium toward the conducting dimers (Fig. 2 *A*). Fig. 2 *B* shows the changes in quench rate at varying concentrations of the three fluoroalcohols and their nonfluorinated counterparts (ethanol, 2-propanol, and *tert*-butanol). The aqueous concentrations at which the alcohols double the fluorescence quench rate are summarized in Table 1. All the tested alcohols altered gramicidin channel function (altered lipid bilayer properties), albeit with different potencies (Fig. 2 *B*; Table 1).

All the alcohols increase the fluorescence quench rate, as would be expected from the thermodynamic bilayer softening associated with the reversible partitioning of amphiphiles into lipid bilayers (53–55).
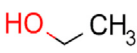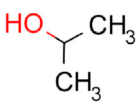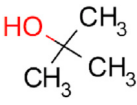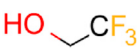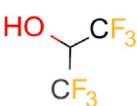
Bilayer-modifying potency

Using the aqueous (nominal) concentrations as reference, PFTB had the greatest effect (the lowest D_{nom}), followed closely by HFIP; both altered the quench rates at low mM concentrations. TFE was the least potent of the three fluoroalcohols but still approximately threefold more bilayer active than its nonfluorinated counterpart ethanol (Table 1). HFIP was so bilayer modifying that it altered lipid bilayer properties when present at only 0.06% [v/v], demonstrating

the importance of removing any HFIP that may have been used as solvent for a molecule of interest.

The rank order of bilayer-modifying potency based on D_{nom} reflects the combined effect of the alcohols' aqueous/bilayer partition coefficients (K_p) and their bilayer-modifying potency per molecule in the membrane. To obtain the mole fractions in the membrane (at aqueous concentration D_{aq}), we determined the alcohols' bilayer partition coefficients by measuring how the fluorescence quench rates varied as function of lipid volume, r_{lip} (see Materials and Methods). The principles underlying the method are described in (38–40). Fig. 3 *A* shows how the normalized fluorescence time courses at 5 mM HFIP (nominal concentration) varied with r_{lip}. The variation in D_{nom} as a function of r_{lip} allows to estimate K_p by fitting Eq. 9 to the D_{nom} vs. r_{lip} relation; Fig. 3 *B* shows results for HFIP. The K_p estimates for all the alcohols are summarized in Table 1. The partition coefficients for the nonfluorinated alcohols are twofold higher than those we used earlier (12); K_p for ethanol is within 20% of the value for $DC_{18:1}PC$ vesicles determined by isothermal titration calorimetry, expressed as the ratio of the ethanol mole fractions in the aqueous solution and the bilayer, and the partition coefficient at 35°C was 71 ± 10 (56), which converts to a K_p 1.4 ± 0.2 when expressed as the ratio of the ethanol concentrations in the two phases (the conversion factor is $[lipid]_{mem}/[H_2O]_{aq}$). We compare the partition coefficients determined using various methods in Fig. S1. Using the estimated mole fraction in the membrane (at aqueous concentration D_{aq}), the fluoroalcohols were similarly or less bilayer modifying than their nonfluorinated counterparts, which are close to equipotent, and the rank order of the fluoroalcohols' potencies was TFE = HFIP > PTFB.

Apart from PFTB, the alcohols' bilayer-modifying potencies per molecule in the bilayer were remarkably similar, with $m_{alc} \approx 0.2$ at $[alc]_{nom} = D$, meaning that, on average, there will be approximately two to four alcohol molecules in the one to two shells of lipids (8–20 lipids) around a

TABLE 1 Properties of the Tested Fluoroalcohols and Their Nonfluorinated Counterparts

Name[a]	Structure[b]	pK_a[c]	D (mM)[d]	K_p[e]	m_{alc}[f]
Ethanol	HO—CH₃	15.9	147 ± 13	1.9 ± 3.3	0.20
2-Propanol	HO—CH₃ / CH₃	16.5	93.3 ± 5.9	4.9 ± 2.4	0.29
tert-Butanol	HO—CH₃ / CH₃ CH₃	16.5	48.3 ± 4.5	7.9 ± 1.3	0.26
TFE	HO—CF₃	12.4	54.3 ± 1.8 (pH 7) 51.9 ± 6.8 (pH 4)	7.2 ± 4.4	0.26
HFIP	HO—CF₃ / CF₃	9.3	5.6 ± 0.4 (pH 7) 7.8 ± 1.0 (pH 4)	66.7 ± 4.9	0.25
PFTB	HO—CF₃ / CF₃ CF₃	5.4	1.4 ± 0.2 (pH 7) 2.1 ± 0.3 (pH 4)	878 ± 10	0.49

[a]Name, alcohol name.
[b]Structures were drawn using MarvinSketch 5.0.3 from ChemAxon (Budapest, Hungary).
[c]pK_a, the logarithmic acid dissociation constant; values from (71) to (72) for the regular and fluoroalcohols, respectively.
[d]D, the concentration $\pm$ fit error (in mM) at which the alcohols double the fluorescence quench rate at pH 7.0 (and also at pH 4.0 for the fluoroalcohols).
[e]K_p, the alcohol bilayer/aqueous phase partition coefficients (K_p) as determined by lipid depletion in the stopped flow assay (mean $\pm$ SD).
[f]m_{alc}, the mole-fraction of alcohol in the bilayer at D.

gramicidin channel (57) when the quench rate has doubled. The number of neighbor alcohols will be higher if there is enrichment due to favorable local-alcohol lateral redistribution in the bilayer deformation area and/or accumulation at the channel/bilayer interface (31,57,58). (Our estimate of m_{alc} at $[alc]_{nom} = D$ is twofold higher than the estimate in (12) because our estimate for K_p is twofold higher than the value used in our earlier study).

Fig. 4 shows comparisons of the alcohols' bilayer-modifying activity, quantified in terms of D_{aq}, with their bilayer partitioning (K_p), as well as how the alcohols' activity, based on their nominal aqueous concentrations and mole fraction in the bilayer, compares to their molecular volumes. Apart from PFTB, the alcohols' bilayer-modifying potency follows their bilayer partitioning in general agreement with the Meyer-Overton correlation (59,60). This is evident in Fig. 4 *A*, in which the red dashed line (excluding PFTB) has a slope closer to one. Accounting for their different partitioning, all the alcohols, except for PFTB, thus have similar bilayer-modifying potencies (Fig. 4 *C*)—and, per molecule in the membrane, there is little difference between

the fluoroalcohols and their nonfluorinated counterparts. This latter result is consistent with the thermodynamic softening associated with the reversible partitioning of amphiphiles into the bilayer (53–55). We further note that, contrary to the results obtained with nicotinic acetylcholine receptors (14), the results for the fluoroalcohols and their nonfluorinated counterparts cannot be combined by using the molecular volume as the descriptor of the alcohols' properties (Fig. 4 *B*).

Knowing the partition coefficients (Table 1) allows us to evaluate how an H → CH₃, a CH₃ → CF₃, or an H → CF₃ substitution in short-chain, branched alcohols alters the partition coefficient between the aqueous phase and the bilayer, as described in Table S2. The results are summarized in Table 2 (equal within experimental errors in the measurements).

Effect of pH

Fluoroalcohols have lower logarithmic acid disassociation constants (pK_as) than their nonfluorinated counterparts
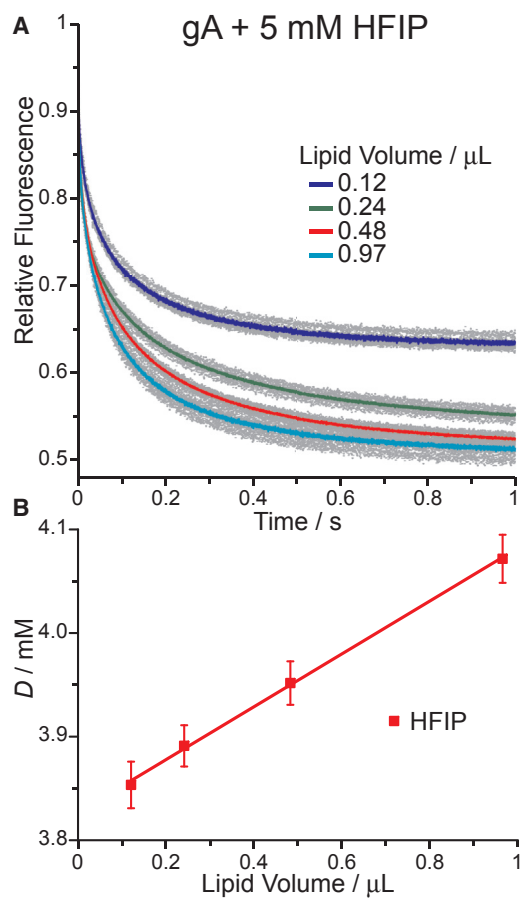
FIGURE 3 Determining the alcohol's bilayer partition coefficients (K_p). The gramicidin-based fluorescence assay was done at different lipid volumes (V_{lip}). (A) Normalized fluorescence time courses observed with fluorophore-loaded LUVs incubated with gramicidin and 5 mM HFIP and varying lipid volumes are shown. (B) The fluorescence quench doubling rate (D_{nom}) for HFIP as function of the lipid volume (of V_{lip}) is shown. To see this figure in color, go online.
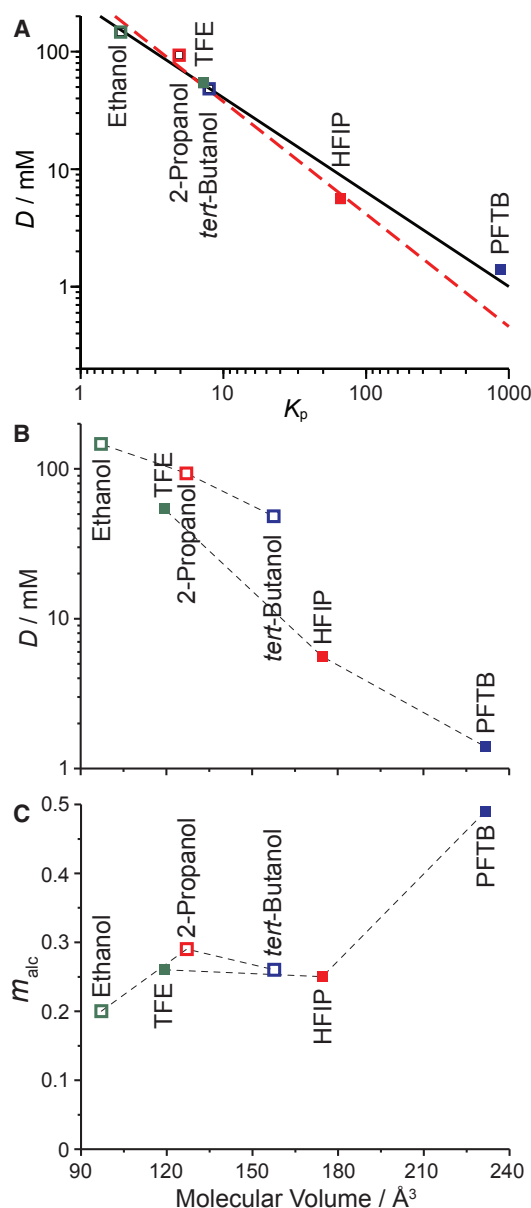

FIGURE 4 Comparison of the alcohol's bilayer perturbing potency at pH 7. (A) D, as determined in Fig. 2, is shown as a function of the alcohol's partition coefficient (K_p). A linear fit (solid line) to the results for all alcohols gives a slope = 0.8, $R^2 = 0.99$. Excluding PFTB (red dashed line), the fit gives a slope close to one; slope = 0.96, $R^2 = 0.99$. (B) D, as determined in Fig. 2, is shown as a function of the molecular volume of the tested fluoroalcohols and their nonfluorinated counterparts. (C) The mole fractions in the bilayer at D (m_{alc}) as a function of molecular volume are shown. To see this figure in color, go online.

(Table 1), and HFIP and PFTB can be considered to be weak acids. (Both the charged and neutral forms of PFTB may partition into the bilayer/solution interface similarly to what is observed for other titratable groups (37)). We therefore explored whether their bilayer-perturbing potencies are pH dependent by determining the dose-response curves at pH 4, at which PFTB (the fluoroalcohol with the lowest pK_a) is mostly deprotonated (Fig. S2). (In the absence of gramicidin, there was little difference in the quench rates observed at pH 4 and 7 (Fig. S3), which demonstrates that Tl^+ does not cross the bilayer as Tl^+-alcoholate ion pairs.) All three fluoroalcohols have similar activities at pH 4 and 7, with HFIP and PFTB being marginally less bilayer active at pH 4 (Table 1).

MD simulations

Straight chain alcohols have been shown—experimentally, in simulations, and in mean-field statistical thermodynamic

analysis—to modulate a range of bilayer physicochemical properties (e.g., (56,61–63), and see Table 1 in (12)). To explore the fluoroalcohols' bilayer interactions at the molecular level, each of the fluoroalcohols and their nonfluorinated counterparts were studied using MD simulations in DOPC bilayers at an m_{alc} of 0.1 (Fig. 5). All the alcohols preferentially localized to the bilayer solution interface, slightly

TABLE 2 Changes in Bilayer Partitioning with the Addition of a Methyl or Trifluoromethyl Group

Substitution[a]	$K_p^{I \rightarrow II} = K_p^{II}/K_p^I$	$\Delta\Delta G_p^{I \rightarrow II} = \Delta\Delta G_p^{II} - \Delta\Delta G_p^{I}$ (kJ/mole)
H → CH$_3$	2.3 ± 0.3	2.1 ± 0.3
CH$_3$ → CF$_3$	4.1 ± 0.6	3.5 ± 0.4
H → CF$_3$	10.1 ± 0.9	5.7 ± 0.2

[a]See Table S2 for calculations.

below the lipid phosphate group (Fig. 5 *B*). The larger, more hydrophobic alcohols localize to somewhat deeper in the bilayer, and the fluoroalcohols tend to reside deeper than their nonfluorinated counterparts, suggesting that they may not be as strongly linked to the bilayer/solution interface as their nonfluorinated counterparts. This is most noticeable for PFTB, which occasionally resides in the bilayer hydrocarbon core, which may account for its lesser bilayer-modifying potency because molecules that are not linked to the interface appear to have less effect on bilayer properties (64). The fluoroalcohols also align slightly more with the bilayer normal than their nonfluorinated counterparts (Fig. S4). The alcohols' effect on bulk bilayer properties at m_{alc} ~0.1 is modest (Table S3), suggesting that any observed changes in membrane protein function are likely to be the result of combination of changes to multiple bilayer properties, consistent with similar comparisons of straight-chain alcohols (58) and phytochemicals (31).

Breakdown of bilayer integrity

At concentrations higher than those tested here using the gramicidin-based fluorescence assay, HFIP and PFTB became overtly bilayer destabilizing and increased the fluorescence quench rate in the absence of gramicidin (seen in Fig. 1 *A* for HFIP), suggesting that HFIP and PTFB at these high concentrations destroy the vesicle integrity. We tested this by monitoring the light absorption of MLVs (prepared from lipids with different acyl chain lengths, C18, C20, and C22) as a function of the fluoroalcohol concentration (Fig. S5). Concentrated MLV solutions are turbid but turn clear if the vesicles are disrupted, either solubilized or precipitated. At the concentrations tested (up to 700 mM), TFE had little effect on light absorption (vesicle integrity); it does, however, disrupt vesicle integrity at an even higher concentration, 50 vol% (19), whereas HFIP and PFTB decreased the light absorption at concentrations above 25 mM (PFTB) and 100 mM (HFIP), respectively. This could suggest that the fluoroalcohols had caused dissolution of vesicles, but on inspection, the lipids were not dissolved but rather had settled as a white precipitate at the bottom of the cuvette. This could suggest that the fluoroalcohols had produced some new lipid phase. We examined this using ^{31}P NMR on MLVs (Fig. 6). When equilibrated with TFE, HFIP, or PFTB at concentrations at which the alcohols did not produce overt bilayer destabilization (20–200 mM, TFE; 10–20 mM, HFIP or PFTB), the fluoroalcohols cause
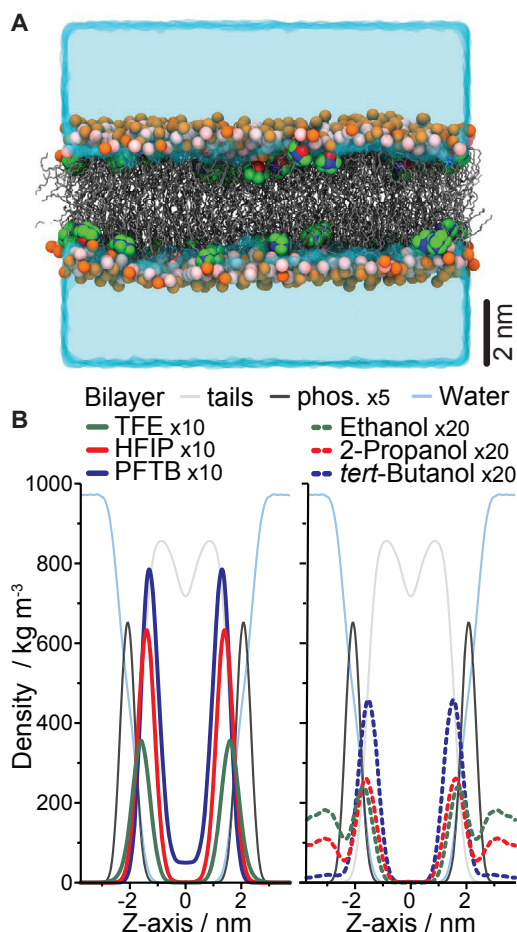

FIGURE 5 The alcohols' position in the bilayer as determined by MD simulations. (*A*) A snapshot from the last frame of an HFIP simulation is shown. All the HFIP molecules are fully imbedded in the DOPC bilayer below the phosphate groups. HFIP is depicted in green, blue, and red for the F, C, and O atoms, respectively. The DOPC lipids are in gray, with their choline and phosphate groups emphasized as orange and pink spheres, respectively. The solvent is rendered as a cyan surface. (*B*) The density of the fluoroalcohols (*left*) and their nonfluorinated counterparts (*right*) is shown along the simulation *z* axes (corresponding to the bilayer normal). The density of water as well as DOPC tails and phosphate atoms are shown for reference. For clarity, select densities are scaled by 5-, 10-, or 20-fold, as indicated. The peak of the phosphate distributions are 2.1 nm from the bilayer center, and the peaks of the alcohol distributions (distance from the bilayer center) are summarized below. Ethanol, 1.7 nm; 2-propanol, 1.6 nm; *tert*-butanol, 1.6 nm; TFE, 1.5 nm; HFIP, 1.4 nm; PFTB, 1.3 nm. To see this figure in color, go online.

only slight shifts in the ^{31}P NMR spectra. At higher HFIP or PFTB concentrations (MLVs equilibrated with 20–200 mM of the fluoroalcohol), the ^{31}P NMR spectra gradually converts from the characteristic bilayer spectrum (65) to an isotropic spectrum, confirming breakdown of bilayer integrity and the presence of a nonbilayer phase. Note that the first evidence for an isotropic phase is seen at 20 mM HFIP, similar to the concentration of HFIP (18 mM) that causes an increased Tl$^+$ flux into the LUVs (Fig. 2). Using dynamic light scattering measurements on LUVs, we found
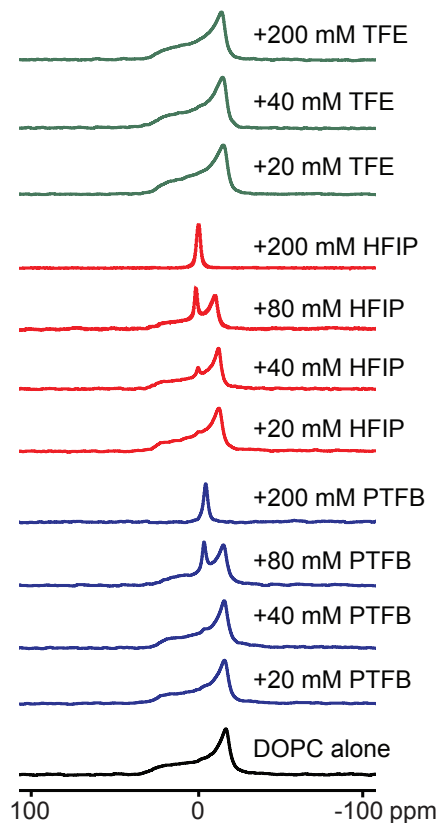
FIGURE 6 Effect of TFE, HFIP, and PFTB on lipid bilayer integrity. ^{31}P NMR spectra on DOPC MLVs were collected in the absence and presence of different concentrations of the fluoroalcohols. With the addition of HFIP and PFTB, the characteristic bilayer spectrum converts to an isotropic spectrum, indicating a breakdown of bilayer integrity. This is first observed in the spectra recorded at 20–40 mM HFIP or PFTB, and the transition is complete at 200 mM HFIP or PFTB. 70 mM NaNO$_3$, 10 mM HEPES (pH 7.0). To see this figure in color, go online.

no evidence for small, micelle-like structures but rather the appearance of aggregates with diameters ~1000 nm, which may suggest that the isotropic phase is a bicontinuous phase.

We did not do ^{31}P NMR experiments on the normal alcohols, but ethanol and butanol are known to stabilize the lamellar phase (66).

CONCLUSIONS

Fluoroalcohols are potent lipid bilayer modifiers, considerably more so than their nonfluorinated counterparts when referenced to the aqueous concentrations (Fig. 2; Table 1) but similar or less so when referenced to the mole fractions in the membrane (Fig. 4). Fluoroalcohols therefore are not just fluorinated probes for their nonfluorinated counterparts. HFIP and PFTB alter gramicidin channel function at low mM concentrations, meaning that experiments using fluoroalcohols or compounds dissolved in fluoroalcohols should include controls for potential bilayer-mediated effects. This becomes especially important for experiments that report

changes in membrane protein function, which may be sensitive to small changes in bilayer properties (30,31).

SUPPORTING MATERIAL

Five figures and three tables are available at http://www.biophysj.org/ biophysj/supplemental/S0006-3495(18)30813-0.

AUTHOR CONTRIBUTIONS

H.I.I. and O.S.A. designed the experiments. M.Z. performed the gA experiments, and M.Z. and H.I.I. analyzed the gA data. I.P., S.J.M., and H.I.I. planned the simulations, and I.P. performed and analyzed them. T.P. performed and analyzed the lipid depletion experiments. D.V.G. performed and analyzed the NMR experiments. M.Z., H.I.I., and O.S.A wrote the manuscript.

ACKNOWLEDGMENTS

SUPPORTING CITATIONS

References (67–70) appear in the Supporting Material.

REFERENCES

1. Bégué, J.-P., D. Bonnet-Delpon, and B. Crousse. 2004. Fluorinated alcohols: a new medium for selective and clean reaction. *Synlett* 18–29.

2. Shuklov, I. A., N. V. Dubrovina, and A. Börner. 2007. Fluorinated alcohols as solvents, cosolvents and additives in homogeneous catalysis. *Synthesis.* 19:2925–2943.

3. Hirota, N., K. Mizuno, and Y. Goto. 1997. Cooperative α-helix formation of β-lactoglobulin and melittin induced by hexafluoroisopropanol. *Protein Sci.* 6:416–421.

4. Hong, D.-P., M. Hoshino, …, Y. Goto. 1999. Clustering of fluorine-substituted alcohols as a factor responsible for their marked effects on proteins and peptides. *J. Am. Chem. Soc.* 121:8427–8433.

5. Barrow, C. J., A. Yasuda, …, M. G. Zagorski. 1992. Solution conformations and aggregational properties of synthetic amyloid β-peptides of Alzheimer's disease. Analysis of circular dichroism spectra. *J. Mol. Biol.* 225:1075–1093.

6. Boden, N., Y. Cheng, and P. F. Knowles. 1997. Equilibrium and non-equilibrium conformations of peptides in lipid bilayers. *Biophys. Chem.* 65:205–210.

7. Michalek, M., E. S. Salnikov, and B. Bechinger. 2013. Structure and topology of the huntingtin 1-17 membrane anchor by a combined solution and solid-state NMR approach. *Biophys. J.* 105:699–710.

8. van den Brink-van der Laan, E., V. Chupin, …, B. de Kruijff. 2004. Small alcohols destabilize the KcsA tetramer via their effect on the membrane lateral pressure. *Biochemistry.* 43:5937–5942.

9. Cantor, R. S. 1999. Lipid composition and the lateral pressure profile in bilayers. *Biophys. J.* 76:2625–2639.

10. Cantor, R. S. 2001. Bilayer partition coefficients of alkanols: predicted effects of varying lipid composition. *J. Phys. Chem. B.* 105:7550–7553.

11. Dopico, A. M., and D. M. Lovinger. 2009. Acute alcohol action and desensitization of ligand-gated ion channels. *Pharmacol. Rev.* 61:98–114.

12. Ingólfsson, H. I., and O. S. Andersen. 2011. Alcohol's effects on lipid bilayer properties. *Biophys. J.* 101:847–855.

13. Weight, F. F., C. Li, and R. W. Peoples. 1999. Alcohol action on membrane ion channels gated by extracellular ATP (P2X receptors). *Neurochem. Int.* 35:143–152.

14. Godden, E. L., R. A. Harris, and T. V. Dunwiddie. 2001. Correlation between molecular volume and effects of n-alcohols on human neuronal nicotinic acetylcholine receptors expressed in Xenopus oocytes. *J. Pharmacol. Exp. Ther.* 296:716–722.

15. Akitake, B., R. E. Spelbrink, …, S. Sukharev. 2007. 2,2,2-Trifluoroethanol changes the transition kinetics and subunit interactions in the small bacterial mechanosensitive channel MscS. *Biophys. J.* 92:2771–2784.

16. Imai, S., M. Osawa, …, I. Shimada. 2012. Functional equilibrium of the KcsA structure revealed by NMR. *J. Biol. Chem.* 287:39634–39641.

17. Lioudyno, M. I., M. Broccio, …, J. E. Hall. 2012. Effect of synthetic aβ peptide oligomers and fluorinated solvents on Kv1.3 channel properties and membrane conductance. *PLoS One.* 7:e35090.

18. Ennaceur, S. M., and J. M. Sanderson. 2005. Micellar aggregates formed following the addition of hexafluoroisopropanol to phospholipid membranes. *Langmuir.* 21:552–561.

19. Ozdirekcan, S., T. K. Nyholm, …, J. A. Killian. 2008. Influence of trifluoroethanol on membrane interfacial anchoring interactions of transmembrane alpha-helical peptides. *Biophys. J.* 94:1315–1325.

20. Capone, R., F. G. Quiroz, …, M. Mayer. 2009. Amyloid-beta-induced ion flux in artificial lipid bilayers and neuronal cells: resolving a controversy. *Neurotox. Res.* 16:1–13.

21. Sokolov, Y., J. A. Kozak, …, J. E. Hall. 2006. Soluble amyloid oligomers increase bilayer conductance by altering dielectric structure. *J. Gen. Physiol.* 128:637–647.

22. Wang, L., Y. Li, …, F. Li. 2014. The effects of organic solvents on the membrane-induced fibrillation of human islet amyloid polypeptide and on the inhibition of the fibrillation. *Biochim. Biophys. Acta.* 1838:3162–3170.

23. O'Connell, A. M., R. E. Koeppe, II, and O. S. Andersen. 1990. Kinetics of gramicidin channel formation in lipid bilayers: transmembrane monomer association. *Science.* 250:1256–1259.

24. Andersen, O. S., C. Nielsen, …, R. E. Koeppe, II. 1999. Ion channels as tools to monitor lipid bilayer-membrane protein interactions: gramicidin channels as molecular force transducers. *Methods Enzymol.* 294:208–224.

25. Harroun, T. A., W. T. Heller, …, H. W. Huang. 1999. Experimental evidence for hydrophobic matching and membrane-mediated interactions in lipid bilayers containing gramicidin. *Biophys. J.* 76:937–945.

26. Lundbaek, J. A., R. E. Koeppe, II, and O. S. Andersen. 2010. Amphiphile regulation of ion channel function by changes in the bilayer spring constant. *Proc. Natl. Acad. Sci. USA.* 107:15427–15430.

27. Andersen, O. S., D. B. Sawyer, and R. E. Koeppe, II. 1992. Modulation of channel function by the host bilayer. *In* Biomembrane Structure and Function. Schenectady. Adenine Press, pp. 227–244.

28. Lundbaek, J. A., P. Birn, …, O. S. Andersen. 2005. Capsaicin regulates voltage-dependent sodium channels by altering lipid bilayer elasticity. *Mol. Pharmacol.* 68:680–689.

29. Søgaard, R., T. M. Werge, …, J. A. Lundbaek. 2006. GABA(A) receptor function is regulated by lipid bilayer elasticity. *Biochemistry.* 45:13118–13129.

30. Rusinova, R., K. F. Herold, …, O. S. Andersen. 2011. Thiazolidinedione insulin sensitizers alter lipid bilayer properties and voltage-dependent sodium channel function: implications for drug discovery. *J. Gen. Physiol.* 138:249–270.

31. Ingólfsson, H. I., P. Thakur, …, O. S. Andersen. 2014. Phytochemicals perturb membranes and promiscuously alter protein function. *ACS Chem. Biol.* 9:1788–1798.

32. Andersen, O. S., M. J. Bruno, …, R. E. Koeppe, II. 2007. Single-molecule methods for monitoring changes in bilayer elastic properties. *Methods Mol. Biol.* 400:543–570.

33. Ingólfsson, H. I., and O. S. Andersen. 2010. Screening for small molecules' bilayer-modifying potential using a gramicidin-based fluorescence assay. *Assay Drug Dev. Technol.* 8:427–436.

34. Ingólfsson, H. I., R. L. Sanford, …, O. S. Andersen. 2010. Gramicidin-based fluorescence assay; for determining small molecules potential for modifying lipid bilayer properties. *J. Vis. Exp.* 44:2131.

35. Berberan-Santos, M. N., E. N. Bodunov, and B. Valeur. 2005. Mathematical functions for the analysis of luminescence decays with underlying distributions 1. Kohlrausch decay function (stretched exponential). *Chem. Phys.* 315:171–182.

36. White, S. H., W. C. Wimley, …, K. Hristova. 1998. Protein folding in membranes: determining energetics of peptide-bilayer interactions. *Methods Enzymol.* 295:62–87.

37. Peitzsch, R. M., and S. McLaughlin. 1993. Binding of acylated peptides and fatty acids to phospholipid vesicles: pertinence to myristoylated proteins. *Biochemistry.* 32:10436–10443.

38. Bruno, M. J., R. E. Koeppe, II, and O. S. Andersen. 2007. Docosahexaenoic acid alters bilayer elastic properties. *Proc. Natl. Acad. Sci. USA.* 104:9638–9643.

39. Ingólfsson, H. I., R. E. Koeppe, II, and O. S. Andersen. 2007. Curcumin is a modulator of bilayer material properties. *Biochemistry.* 46:10384–10391.

40. Heerklotz, H., and S. Keller. 2013. How membrane partitioning modulates receptor activation: parallel versus serial effects of hydrophobic ligands. *Biophys. J.* 105:2607–2610.

41. Miller, R. G. 1974. The jackknife-a review. *Biometrika.* 61:1–15.

42. Pronk, S., S. Páll, …, E. Lindahl. 2013. GROMACS 4.5: a high-throughput and highly parallel open source molecular simulation toolkit. *Bioinformatics.* 29:845–854.

43. Oostenbrink, C., A. Villa, …, W. F. van Gunsteren. 2004. A biomolecular force field based on the free enthalpy of hydration and solvation: the GROMOS force-field parameter sets 53A5 and 53A6. *J. Comput. Chem.* 25:1656–1676.

44. Malde, A. K., L. Zuo, …, A. E. Mark. 2011. An automated force field topology builder (ATB) and repository: version 1.0. *J. Chem. Theory Comput.* 7:4026–4037.

45. Berendsen, H. J. C., J. P. M. Postma, …, J. Hermans. 1981. Interaction models for water in relation to protein hydration. *In* Intermolecular Forces. B. Pullman, ed. Reidel, pp. 331–342.

46. Berendsen, H. J. C., and J. P. M. Postma. 1984. Molecular dynamics with coupling to an external bath. *J. Chem. Phys.* 81:3684–3690.

47. Darden, T., D. York, and L. Pedersen. 1993. Particle mesh Ewald: an N·log(N) method for Ewald sums in large systems. *J. Chem. Phys.* 98:10089–10092.

48. Hess, B., H. Bekker, …, J. G. E. M. Fraaije. 1997. LINCS: a linear constraint solver for molecular simulations. *J. Comput. Chem.* 18:1463–1472.

49. Avramovic-Zikic, O., and K. Colbow. 1978. Turbidity changes of lipid vesicles near the phase transition temperature as an indication of fusion. *Biochim. Biophys. Acta.* 512:97–104.

50. Meyuhas, D., S. Nir, and D. Lichtenberg. 1996. Aggregation of phospholipid vesicles by water-soluble polymers. *Biophys. J.* 71:2602–2612.

51. Wang, A., C. C. Miller, and J. W. Szostak. 2018. Interpreting turbidity measurements for vesicle studies. *bioRxiv* https://doi.org/10.1101/348904.

52. Martinus, N., and C. A. Vincent. 1976. Viscosity of aqueous solutions of TlNO3, Tl2SO4 and TlOH at 25°C. *J. Chem. Soc., Faraday Trans. I.* 72:2505–2511.

53. Evans, E., W. Rawick, and A. F. Hofmann. 1995. Lipid bilayer expansion and mechanical disruption in solutions of water-soluble bile acid. *In* Bile Acids in Gastroenterology Basic and Clinical Advances. A. Hofmann, G. Paumgartner, and A. Stiehl, eds. Kluwer Academic, pp. 59–68.

54. Zhelev, D. V. 1998. Material property characteristics for lipid bilayers containing lysolipid. *Biophys. J.* 75:321–330.

55. Bruno, M. J., R. Rusinova, …, O. S. Andersen. 2013. Interactions of drugs and amphiphiles with membranes: modulation of lipid bilayer elastic properties by changes in acyl chain unsaturation and protonation. *Faraday Discuss.* 161:461–480, discussion 563–589.

56. Terama, E., O. H. Ollila, …, I. Vattulainen. 2008. Influence of ethanol on lipid membranes: from lateral pressure profiles to dynamics and partitioning. *J. Phys. Chem. B.* 112:4131–4139.

57. Beaven, A. H., A. M. Maer, …, W. Im. 2017. Gramicidin A channel formation induces local lipid redistribution I: experiment and simulation. *Biophys. J.* 112:1185–1197.

58. Melo, M. N., C. Arnarez, …, H. I. Ingólfsson. 2017. High-throughput simulations reveal membrane-mediated effects of alcohols on MscL gating. *J. Am. Chem. Soc.* 139:2664–2671.

59. Meyer, H. 1901. Zur Theorie der Alkoholnarkose. *Naunyn Schmiedebergs Arch. Pharmacol.* 46:338–346.

60. Overton, C. E. 1901. Studien über die Narkose zugleich ein Beitrag zur allgemeinen Pharmakologie. Gustav Fischer, Jena, Germany.

61. Cantor, R. S. 2001. Breaking the Meyer-Overton rule: predicted effects of varying stiffness and interfacial activity on the intrinsic potency of anesthetics. *Biophys. J.* 80:2284–2297.

62. Griepernau, B., and R. A. Böckmann. 2008. The influence of 1-alkanols and external pressure on the lateral pressure profiles of lipid bilayers. *Biophys. J.* 95:5766–5778.

63. Stetter, F. W., and T. Hugel. 2013. The nanomechanical properties of lipid membranes are significantly influenced by the presence of ethanol. *Biophys. J.* 104:1049–1055.

64. Dockendorff, C., D. M. Gandhi, …, J. T. Sack. 2018. Synthetic analogues of the snail toxin 6-bromo-2-mercaptotryptamine dimer (BrMT) reveal that lipid bilayer perturbation does not underlie its modulation of voltage-gated potassium channels. *Biochemistry.* 57:2733–2743.

65. de Kruijff, B., P. R. Cullis, …, T. F. Taraschi. 1985. Lipid polymorphism and membrane function. *In* The Enzymes of Biological Membranes: Volume 1 Membrane Structure and Dynamics. A. N. Martonosi, ed. Springer, pp. 131–204.

66. Tilcock, C. P., and P. R. Cullis. 1987. Lipid polymorphism. *Ann. N. Y. Acad. Sci.* 492:88–102.

67. Petrauskas, A., and E. Kolovanov. 2000. ACD/Log P method description. *Perspect. Drug Discov. Des.* 19:99–116.

68. Cheng, T., Y. Zhao, …, L. Lai. 2007. Computation of octanol-water partition coefficients by guiding an additive model with knowledge. *J. Chem. Inf. Model.* 47:2140–2148.

69. Abraham, M. H., H. S. Chadha, …, R. C. Mitchell. 1994. Hydrogen bonding. 32. An analysis of water-octanol and water-alkane partitioning and the delta log P parameter of seiler. *J. Pharm. Sci.* 83:1085–1100.

70. Hansch, C., A. Leo, and D. H. Hoekman. 1995. Exploring QSAR: Hydrophobic, Electronic, and Steric Constants. American Chemical Society, Washington, DC.

71. Reeve, W., C. M. Erikson, and P. F. Aluotto. 1979. A new method for the determination of the relative acidities of alcohols in alcoholic solutions. The nucleophilicities and competitive reactivities of alkoxides and phenoxides. *Can. J. Chem.* 57:2747–2754.

72. Donghi, D., T. Beringhelli, …, M. Mondini. 2006. NMR investigation of the dihydrogen-bonding and proton-transfer equilibria between the hydrido carbonyl anion [HRe2(CO)9]- and fluorinated alcohols. *Chemistry.* 12:1016–1025.